Light (anti-)nuclei production and flow in relativistic heavy-ion collisions

Lilin Zhu,[1,*] Che Ming Ko,[2,†] and Xuejiao Yin[1,‡]
[1]*Department of Physics, Sichuan University, Chengdu 610064, China*
[2]*Cyclotron Institute and Department of Physics and Astronomy, Texas A&M University, College Station, Texas 77843, USA*
(Received 13 October 2015; revised manuscript received 10 November 2015; published 28 December 2015)

Using the coalescence model based on the phase-space distributions of protons, neutrons, Λs, and their antiparticles from a multiphase transport (AMPT) model, we study the production of light nuclei (^{2}H, ^{3}H, ^{3}He, $^3_\Lambda$H) and their antinuclei in Pb+Pb collisions at $\sqrt{s_{NN}} = 2.76$ TeV. The resulting transverse momentum spectra, elliptic flows, and coalescence parameters for these nuclei are presented and compared with available experimental data. We also show the constituent number scaled elliptic flows of these nuclei and discuss its implications.

DOI: 10.1103/PhysRevC.92.064911 PACS number(s): 25.75.Nq, 25.75.Ld

I. INTRODUCTION

Recently, light nuclei production has been studied at the Large Hadron Collider (LHC) by the ALICE Collaboration [1,2]. Similar to the experiments carried out earlier by the STAR Collaboration at the Relativistic Heavy Ion Collider (RHIC) [3–6], the motivation for such studies is twofold. One part is to search for nuclei that do not exist in nature in order to study if nuclei and antinuclei have same properties and to discover the stability of multistrange hypernuclei and antinuclei. Indeed, it was in heavy-ion collisions that anti-hypernuclei were discovered by the STAR Collaboration [5]. The other part is to use light nuclei to study the space-time structure of the emission source in relativistic heavy-ion collisions since they are likely produced at kinetic freeze-out via nucleon coalescence, complementing the method using the Hanbury-Brown Twiss (HBT) interferometry [7,8] of particles emitted at freeze-out. The use of the coalescence model for studying light nuclei production has a long history with applications in heavy-ion collisions at both intermediate [9–12] and high energies [13,14] as well as at relativistic energies [15–19]. In most applications of the coalescence model, the energy spectra for light nuclei are simply given by the product of the spectra of their constituent nucleons multiplied by empirical coalescence parameters. In a more sophisticated coalescence model, the coalescence parameter is computed from the overlap of the nuclear Wigner phase-space density with the nucleon phase-space distributions at freeze-out. For example, in Refs. [20,21], the authors used the phase-space distributions of nucleons at freeze-out from an isospin-dependent transport model for heavy-ion collisions at intermediate energies with radiative beams to study production of light nuclei such as deuteron, triton, helium-3, and α particles in the coalescence model. It was found in this study that the yield of light nuclei is sensitive to the density dependence of nuclear symmetry energy. Also, the study of deuteron production in heavy-ion collisions at RHIC was studied in Ref. [22] based on a multiphase transport (AMPT) model. Both the coalescence model based on the phase-space distributions of protons and neutrons at freeze-out and a dynamic model that includes deuteron production and annihilation via $NN \leftrightarrow \pi d$ in the hadronic stage of AMPT have been used. It was found that the final deuteron yield and elliptic flow from these two approaches are similar, providing thus a consistent check on the applicability of the coalescence model to deuteron production in heavy-ion collisions. In the present study, we extend the study of Ref. [22] to include the production of not only deuteron (^{2}H) but also triton (^{3}H), helium-3 (^{3}He), and hypertriton ($^3_\Lambda$H) as well as their antinuclei from the coalescence model using the phase-space distributions of protons, neutrons, Λs, and their antiparticles at freeze-out from the AMPT model in both its default and string melting versions. We specifically study the transverse momentum spectra and elliptic flows of these nuclei for Pb+Pb collisions at $\sqrt{s_{NN}} = 2.76$ TeV as studied in the experiments by the ALICE Collaboration. We also determine the coalescence parameters from the transverse momentum spectra of these nuclei.

The paper is organized as follows. In Sec. II, we briefly review the AMPT model used for the present study. The coalescence model is then described in Sec. III. In Sec. IV, we show results from our study on the transverse momentum spectra, elliptic flows, and coalescence parameters for ^{2}H, ^{3}H, ^{3}He, and $^3_\Lambda$H as well as their antinuclei. Finally, a summary is given in Sec. V.

II. THE AMPT MODEL

To obtain the phase-space distributions of protons, neutrons, and Λs as well as their antiparticles, we use the AMPT model that has been extensively utilized for studying heavy-ion collisions at relativistic energies. The AMPT model is a hybrid model [23] with the initial particle distributions generated by the heavy-ion jet interaction generator (HIJING) model [24]. In the default version, the jet quenching in the HIJING model is replaced in the AMPT model by explicitly taking into account the scattering of minijet partons via Zhang's parton cascade (ZPC) model [25]. These partons are recombined with their parent strings after their scattering, which are then converted to hadrons using the Lund string fragmentation model. In the

*zhulilin@scu.edu.cn
†ko@comp.tamu.edu
‡yinxuejiao@stu.scu.edu.cn

version of string melting, all hadrons produced from string fragmentation in the HIJING model are converted to their valence quarks and antiquarks, whose evolution in time and space is modeled by the ZPC model. After the end of their scatterings, quarks and antiquarks are converted to hadrons via a spatial coalescence model. In both versions of the AMPT model, the scatterings among hadrons are described by a relativistic transport (ART) model [26]. In the present study, we adopt the version Ampt-v1.25t7–v2.25t7[1] with the default Lund string fragmentation parameters $a = 0.5$ and $b = 0.9$ GeV^{-2} in the HIJING model, the QCD coupling constant $\alpha_s = 0.33$, and the screening mass $\mu = 3.2$ fm^{-1} to obtain a parton scattering cross section of 1.5 mb in ZPC. These parameters were shown in Ref. [27] to give a better description of both the charged particle multiplicity density at midrapidity and elliptic flow measured in heavy-ion collisions at the LHC than their values used in Ref. [23] for heavy-ion collisions at RHIC.

III. THE COALESCENCE MODEL

For light nuclei production in heavy-ion collisions, both the statistical model [28,29], which assumes that light nuclei are in both thermal and chemical equilibrium with all other particles in the produced hot dense matter, and the coalescence model have been used. In the present study, we use the coalescence model to study light nuclei production based on the phase-space distributions of protons, neutrons, and Λs as well as their antiparticles at freeze-out from the AMPT model described in the previous section.

The coalescence model for nuclei production in heavy-ion collisions is based on the sudden approximation of projecting out their wave functions from the wave functions of nucleons at freeze-out. As shown in Ref. [13], the number of nuclei consisting of A constituents produced in a heavy-ion collision is then given by the overlap integral of the Wigner function $f_A(\mathbf{x}'_1,\ldots,\mathbf{x}'_A;\mathbf{p}'_1,\ldots,\mathbf{p}'_A)$ of the produced nucleus with the phase-space distribution function $f_N(\mathbf{x},\mathbf{p})$ of the constituents at freeze-out, which is normalized to the constituent number N according to $\int d^3\mathbf{x}d^3\mathbf{p}\, f_N(\mathbf{x},\mathbf{p}) = N$, that is,

$$\frac{dN_A}{d^3\mathbf{P}_A} = g_A \int \Pi_{i=1}^{A} d^3\mathbf{x}_i d^3\mathbf{p}_i\, f_N(\mathbf{x}_i,\mathbf{p}_i) \times f_A(\mathbf{x}'_1,\ldots,\mathbf{x}'_A;\mathbf{p}'_1,\ldots,\mathbf{p}'_A)\delta^{(3)}\left(\mathbf{P}_A - \sum_{i=1}^{A}\mathbf{p}_i\right), \tag{1}$$

where $g_A = (2J_A+1)/2^A$ is the statistical factor for A constituents of spin 1/2 to form a nucleus of angular momentum J_A. As in Refs. [21,22], the coordinate $\mathbf{x}_i$ and momentum $\mathbf{p}_i$ are those of the ith constituent in the center-of-mass of colliding heavy ions when it freezes out, i.e., undergoes its last scattering. The corresponding coordinate $\mathbf{x}'_i$ and momentum $\mathbf{p}'_i$, which appears in the nuclear Wigner function, are obtained by first Lorentz transforming to the rest frame of produced nucleus and then letting this constituent propagate freely with a constant velocity, given by the ratio of its momentum and energy in the rest frame of the nucleus, until the time when the last constituent in the nucleus freezes out.

For the light nuclei we consider in this study, such as ^{2}H, ^{3}H, ^{3}He, $^3_\Lambda$H, and their antinuclei, we approximate their wave functions by those of the ground state of a harmonic oscillator with the oscillator constant adjusted to fit the empirical charge radii of these nuclei. The Wigner function for a nucleus consisting of two constituents is then [30]

$$f_2(\boldsymbol{\rho},\mathbf{p}_\rho) = 8g_2 \exp\left[-\frac{\boldsymbol{\rho}^2}{\sigma_\rho^2} - \mathbf{p}_\rho^2\sigma_\rho^2\right], \tag{2}$$

where

$$\boldsymbol{\rho} = \frac{1}{\sqrt{2}}(\mathbf{x}'_1 - \mathbf{x}'_2), \quad \mathbf{p}_\rho = \sqrt{2}\frac{m_2\mathbf{p}'_1 - m_1\mathbf{p}'_2}{m_1+m_2}, \tag{3}$$

with m_i, $\mathbf{x}'_i$, and $\mathbf{p}'_i$ being the mass, position, and momentum of constituent i, respectively.

Similarly, the Wigner function for a nucleus consisting of three constituents is [30]

$$f_3(\boldsymbol{\rho},\boldsymbol{\lambda},\mathbf{p}_\rho,\mathbf{p}_\lambda) = 8^2 g_3 \exp\left[-\frac{\boldsymbol{\rho}^2}{\sigma_\rho^2} - \frac{\boldsymbol{\lambda}^2}{\sigma_\lambda^2} - \mathbf{p}_\rho^2\sigma_\rho^2 - \mathbf{p}_\lambda^2\sigma_\lambda^2\right], \tag{4}$$

where $\boldsymbol{\rho}$ and $\mathbf{p}_\rho$ are similarly defined as in Eq. (3), and

$$\boldsymbol{\lambda} = \sqrt{\frac{2}{3}}\left(\frac{m_1\mathbf{x}'_1 + m_2\mathbf{x}'_2}{m_1+m_2} - \mathbf{x}'_3\right),$$
$$\mathbf{p}_\lambda = \sqrt{\frac{3}{2}}\frac{m_3(\mathbf{p}'_1+\mathbf{p}'_2) - (m_1+m_2)\mathbf{p}'_3}{m_1+m_2+m_3}. \tag{5}$$

The width parameter σ_ρ in Eq. (2) is related to the charge mean-square radius of the nucleus of two constituents via [30]

$$\langle r_2^2\rangle = 3\frac{|Q_1m_2^2 + Q_2m_1^2|}{(m_1+m_2)^2}\sigma_\rho^2 = \frac{3}{2}\frac{|Q_1m_2^2 + Q_2m_1^2|}{\omega m_1m_2(m_1+m_2)}, \tag{6}$$

where the second line follows if we use the relation $\sigma_\rho = 1/\sqrt{\mu_1\omega}$ in terms of the oscillator frequency ω in the harmonic oscillator wave function and the reduced mass $\mu_1 = 2(1/m_1 + 1/m_2)^{-1}$.

For the width parameter σ_λ in Eq. (4), it is related to the oscillator frequency by $(\mu_2\omega)^{-1/2}$, with $\mu_2 = (3/2)[1/(m_1+m_2) + 1/m_3]^{-1}$. Its value and also that of $\sigma_\rho = 1/\sqrt{\mu_1\omega}$ are then determined from the oscillator constant via the mean-square charge radius of the nucleus of three constituents,

[1]This version was downloaded from http://myweb.ecu.edu/linz/ampt and run with a modified file linana.f to change the coalescence order between mesons and baryons.

that is [30]

$$\langle r_3^2 \rangle = \frac{3}{2} \frac{|Q_1 m_2 m_3 (m_2 + m_3) + Q_2 m_3 m_1 (m_3 + m_1) + Q_3 m_1 m_2 (m_1 + m_2)|}{\omega m_1 m_2 m_3 (m_1 + m_2 + m_3)}. \quad (7)$$

IV. RESULTS

In the present section, we show results on the transverse momentum spectra, elliptic flows, and coalescence parameters for ^{2}H, ^{3}H, ^{3}He, and $^3_\Lambda$H as well as their antinuclei. They are calculated from the coalescence model using the phase-space distributions of proton, neutron, Λ, and their antiparticles at freeze-out from the AMPT model. For ^{2}H, ^{3}H, and ^{3}He, their statistical factors and the values of the width parameters in their Wigner functions are shown in Table I together with the empirical values of their charge radii and the resulting oscillator constants. Same parameters are used for their antinuclei. For $^3_\Lambda$H and $^3_{\bar\Lambda}\bar{\rm H}$, they are assumed to have same properties as corresponding nuclei of three nucleons, and the width parameters in their Wigner functions are thus taken to be the same as those for ^{3}H.

Since the hot dense matter produced at the midrapidity of Pb+Pb collisions at $\sqrt{s_{NN}} = 2.76$ TeV is essentially baryon free and has zero isospin, the distributions of protons and neutrons as well as their antiparticles are similar. Therefore, ^{2}H and $^2\bar{\rm H}$ also have similar distributions. The same is true for the distributions of ^{3}H, ^{3}He, and their antinuclei as well as those of $^3_\Lambda$H and $^3_{\bar\Lambda}\bar{\rm H}$. Furthermore, to improve the statistics of the results for $^3_\Lambda$H and $^3_{\bar\Lambda}\bar{\rm H}$, we have also calculated the distributions of $^3_\Lambda$He and $^3_\Lambda n$ as well as their antinuclei, assuming that the width parameters of their Wigner functions are the same as those for ^{3}He and ^{3}H, respectively, although $^3_\Lambda$He has not been observed and $^3_\Lambda n$ has only been seen in one experiment [32]. In the following, we thus show results that are obtained by averaging over these similar distributions, i.e., $(p + n + \bar p + \bar n)/4$, $(\Lambda + \bar\Lambda)/2$, $(^2{\rm H} + ^2\bar{\rm H})/2$, $(^3{\rm H} + ^3{\rm He} + ^3\bar{\rm H} + ^3\overline{\rm He})/4$, and $(^3_\Lambda{\rm H} + ^3_\Lambda{\rm He} + ^3_\Lambda n + ^3_{\bar\Lambda}\bar{\rm H} + ^3_{\bar\Lambda}\overline{\rm He} + ^3_{\bar\Lambda}\bar n)/6$, and they are denoted in the following as N-like, Λ-like, ^{2}H-like, ^{3}H-like and $^3_\Lambda$H-like, respectively.

A. Transverse momentum spectra

In Fig. 1, we show the transverse momentum spectra of N-like (solid line), Λ-like (dashed line), ^{2}H-like (dash-dotted line), ^{3}H-like (filled triangles), and $^3_\Lambda$H-like (open triangles) at midrapidity from the default (left panel) and the string melting (right panel) AMPT model for Pb+Pb collisions at $\sqrt{s_{NN}} = 2.76$ TeV and impact parameter $b = 8$ fm. Also shown in the figure are the proton (open diamonds) and deuteron (open squares) transverse momentum spectra from the ALICE Collaboration [1] for collisions at centralities 20–30% and 20–40%, respectively, which are similar to collisions at impact parameter $b = 8$ fm used in the AMPT calculations. It is seen that the default AMPT model describes reasonably the experimentally measured proton transverse momentum spectrum but overestimates that of deuteron. The string melting AMPT model overestimates, however, both measured proton and deuteron transverse momentum spectra. The latter is not surprising as it has already been pointed out in Ref. [23] that baryons are not properly described by the AMPT with string melting, giving generally a larger number and a soft transverse momentum spectrum at midrapidity, because of the way AMPT treats baryon production via quark coalescence at hadronization. Although some improvements on the problem have been introduced in the version of AMPT code used in the present study by changing the coalescence order between mesons and baryons, this has apparently not solved the problem. Further improvements are thus needed in the AMPT model.

The total number of light nuclei produced in a collision can be obtained from integrating their transverse momentum spectra. For the default AMPT model, the numbers are 24 for N-like, 16 for Λ-like, 0.36 for ^{2}H-like, 8.6×10^{-4} for ^{3}H-like, and 5.5×10^{-4} for $^3_\Lambda$H-like, while for the string melting AMPT model, the corresponding numbers are 38, 21, 2.1, 2.4×10^{-2}, and 2.5×10^{-2}, respectively. The penalty in adding a nucleon

TABLE I. Statistical factor (g), root-mean-square charge radius ($R_{\rm ch}$), oscillator frequency (ω), and width parameter (σ_ρ, σ_λ) for deuteron (^{2}H), triton (^{3}H), and helium-3 (^{3}He). Radii are taken from Ref. [31].

Nucleus	g	$R_{\rm ch}$ (fm)	ω (s^{-1})	σ_ρ,σ_λ (fm)
^{2}H	3/4	2.1421	0.1739	2.473
^{3}H	1/4	1.7591	0.3438	1.759
^{3}He	1/4	1.9661	0.5504	1.390

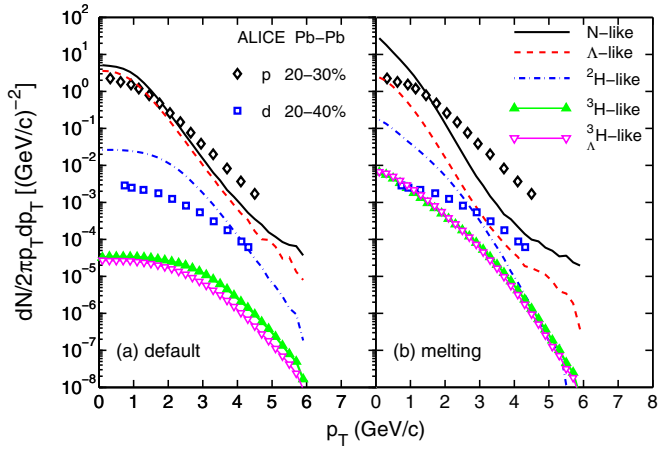

FIG. 1. (Color online) Transverse momentum spectra of N-like (solid line), Λ-like (dashed line), and ^{2}H-like (dash-dotted line), ^{3}H-like (filled triangles), $^3_\Lambda$H-like (open triangles) at midrapidity $|y| \leqslant 0.5$ from the default (left panel) and the string melting (right panel) AMPT model for Pb+Pb collisions at $\sqrt{s_{NN}} = 2.76$ TeV and impact parameter $b = 8$ fm. Data for protons (open diamonds) and deuterons (open squares) are from the ALICE Collaboration [1,2].

to form a heavier nucleus is thus about two orders of magnitude smaller in both the default and the string melting AMPT model, similar to that found in experimental data. Because the number of nuclei produced from coalescence is much smaller than the number of nucleons and Λs, the errors introduced in the coalescence model by allowing a nucleon or Λ to coalescence with many other nucleons and Λs are thus negligibly small.

Since ^{2}H is known to have a small mixture of D waves in its wave function (∼5%), which results in a hole in its density distribution at the center, we have estimated this effect on the yield of ^{2}H and $^2\bar{\text{H}}$ using the D-wave Winger function in Ref. [33]. We have found that this only leads to a reduction of their number by about 3% in both default and string melting AMPT if the D-wave component in the deuteron is taken to be 5%. This effect is negligible in view of the uncertainties in the accuracy of the AMPT in describing the dynamics of a heavy-ion collisions, particularly in the case of the string melting version as mentioned above.

In our study, we have ignored the possible dissociation of light nuclei produced from coalescence of nucleons at freeze-out by freeze-out pions. Because of the large pion-pion elastic scattering cross section, which has a peak value of 175 mb due to the ρ meson resonance [34], the dissociation of light nuclei by pions is then negligible if their dissociation cross sections are smaller than 175 mb. This is indeed the case for the deuteron because its dissociation cross section by a pion via the reaction $d\pi \to NN$ has a peak value of only 10 mb due to the Δ resonance [35,36]. For other light nuclei considered in the present study, their dissociation cross section by pions would be even smaller because their size is smaller than that of the deuteron. Including dissociation of light nuclei by pions is thus not expected to affect our results much. However, because of their small dissociation cross sections, light nuclei might even be produced before nucleons freeze out. This seems to be the case as shown in Fig. 6 of Ref. [22], where the times for deuteron production in the transport approach via the reactions $pp \leftrightarrow d\pi$ are seen to be earlier than those for deuteron production from the coalescence of nucleons at freeze-out, although the difference is not large. Since including the production of light nuclei with more than two nucleons in the transport approach are technically challenging and have not yet been done, we postpone such a study for the future.

B. Elliptic flows

The momentum distribution of nucleus A produced in a heavy-ion collision event can be generally written as

$$f_A(p_T,\phi,y) = \frac{N_A(p_T,y)}{2\pi}\left\{1+2\sum_n v_n(p_T,y)\cos[n(\phi-\Psi_n)]\right\}, \quad (8)$$

where ϕ is the azimuthal angle, Ψ_n is the nth-order event plane angle, and $N_A(p_T,y)$ and $v_n(p_T,y)$ are the number of nuclei of transverse momentum p_T at rapidity y and their nth-order anisotropic flows, respectively. In the present study, we are only interested in the elliptic flow v_2. Also, we neglect the fluctuation of event plane angle Ψ_2 by taking $\Psi_2 = 0$ as our calculations involve the mixing of many events to reduce the statistical fluctuations due to the small number of nucleons and Λs in an event. In this case, the elliptic flow can be simply calculated from

$$v_2(p_T) = \left\langle \frac{p_x^2 - p_y^2}{p_x^2 + p_y^2} \right\rangle, \quad (9)$$

where $\langle\cdots\rangle$ indicates average over all nuclei A in all events.

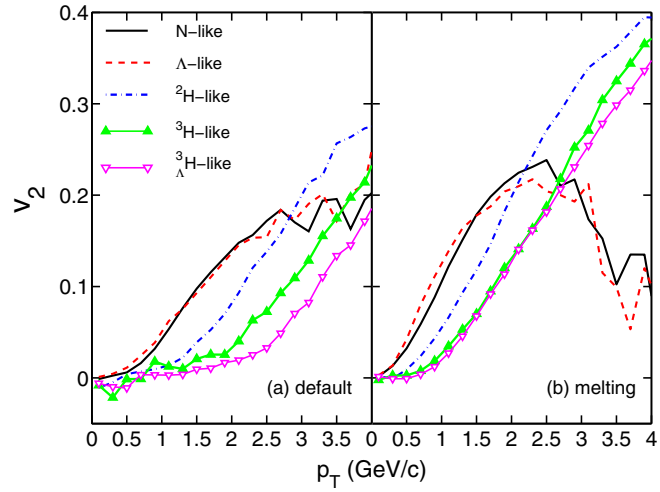

FIG. 2. (Color online) Elliptic flows of N-like (solid line), Λ-like (dashed line), ^{2}H-like (dash-dotted line), ^{3}H-like (filled triangles), and $^3_\Lambda$H-like (open triangles) at midrapidity $|y| \leqslant 0.5$ from the default (left panel) and the string melting (right panel) AMPT model for Pb+Pb collisions at $\sqrt{s_{NN}} = 2.76$ TeV and impact parameter $b = 8$ fm.

Figure 2 shows the elliptic flow of N-like (solid line), Λ-like (dashed line), ^{2}H-like (dash-dotted line), ^{3}H-like (filled triangles), and $^3_\Lambda$H-like (open triangles) at midrapidity $|y| \leqslant 0.5$ from the default (left panel) and the string melting (right panel) AMPT model for Pb+Pb collisions at $\sqrt{s_{NN}} = 2.76$ TeV and impact parameter $b = 8$ fm. These results are obtained from 40 000 AMPT default or string melting events with the mixing of 50 events in calculating the elliptic flows of light (anti-)nuclei. Both the N-like and the Λ-like are seen to have similar elliptic flows in both the default and the string melting AMPT model. Also, as the nuclei get heavier, their elliptic flow becomes smaller, similar to the mass ordering of elliptic flows seen in the hydrodynamic description of collective flow. Because of the strong partonic scattering, the elliptic flow of nuclei is larger in the string melting version of AMPT than in the default version.

A unique feature of the coalescence model is its prediction of an approximate constituent number scaling of the elliptic flows of nuclei, which states that the elliptic flow of a nucleus at transverse momentum p_T per constituent is the same as a function of p_T divided by the number of constituents [37,38]. For light nuclei considered here, $v_2^A(p_T/A)/A$ is then the same. This scaling would be exact if only constituents of same momentum can coalescence to form a nucleus, corresponding to a width parameter in the Wigner function of the nucleus that is infinitely large [39].

Figure 3 shows the constituent number scaled elliptic flow of N-like (solid line), Λ-like (dashed line), ^{2}H-like

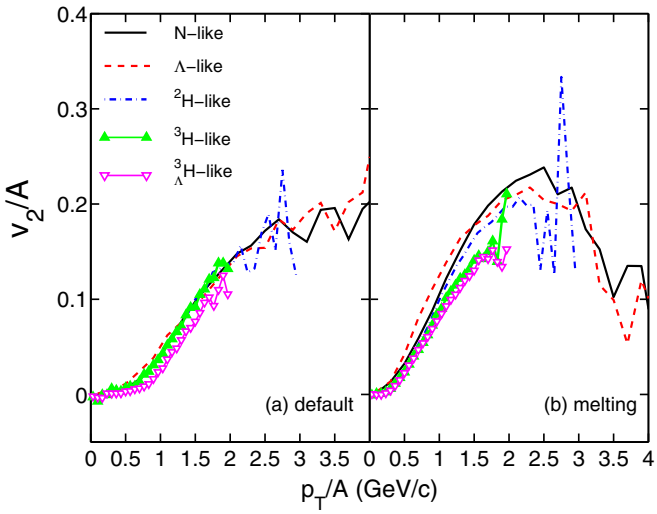

FIG. 3. (Color online) Constituent number scaled elliptic flows of N-like (solid line), Λ-like (dashed line), ^{2}H-like (dash-dotted line), ^{3}H-like (filled triangles), and $^3_\Lambda$H-like (open triangles) at midrapidity $|y| \leqslant 0.5$ from the default (left panel) and the string melting (right panel) AMPT model for Pb+Pb collisions at $\sqrt{s_{NN}} = 2.76$ TeV and impact parameter $b = 8$ fm.

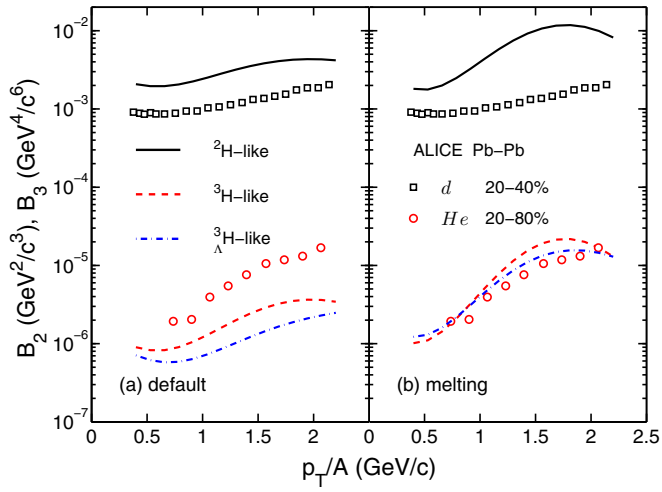

FIG. 4. (Color online) Coalescence parameters for ^{2}H-like (solid line), ^{3}H-like (dashed line), and $^3_\Lambda$H-like (dash-dotted line) at midrapidity $|y| \leqslant 0.5$ from the default (left panel) and the string melting (right panel) AMPT model for Pb+Pb collisions at $\sqrt{s_{NN}} = 2.76$ TeV and impact parameter $b = 8$ fm. Data for B_2 (open squares) and B_3 (open circles) are from the ALICE Collaboration [1,2].

(dash-dotted line), ^{3}H-like (filled triangles), and $^3_\Lambda$H-like (open triangles) at midrapidity $|y| \leqslant 0.5$ from the default (left panel) and the string melting (right panel) AMPT model for Pb+Pb collisions at $\sqrt{s_{NN}} = 2.76$ TeV and impact parameter $b = 8$ fm. It indeed shows that the scaled elliptic flows of all light nuclei are similar in the default AMPT model, although there are some deviations in the case of the string melting AMPT model, which may again be related to the baryon problem in this model, as discussed above. We note that an approximate nucleon number scaling of the elliptic flows of light nuclei was also obtained in heavy-ion collisions at intermediate energies in a study based on the quantum molecular dynamics (QMD) model [40].

C. Coalescence parameters

Results from the coalescence model can be characterized by the coalescence parameter B_A defined via the relation

$$E_A \frac{d^3N_A}{d\mathbf{p}_A^3} = B_A \left(E_p \frac{d^3N_p}{d\mathbf{p}_p^3} \right)^A, \tag{10}$$

where $\mathbf{p}_A$ and $\mathbf{p}_p$ are the momenta of the nucleus and the coalescence constituent, respectively. Using $d^3\mathbf{p}/E = dyd^2p_T$, the above equation can be written as

$$\frac{d^3N_A}{dyd^2p_{TA}} = B_A \left(\frac{d^3N_p}{dy_p d^2p_{Tp}} \right)^A. \tag{11}$$

In Fig. 4, we show the coalescence parameters for ^{2}H-like (solid line), ^{3}H-like (dashed line), and $^3_\Lambda$H-like (dash-dotted line) at midrapidity $|y| \leqslant 0.5$ from the default (left panel) and the string melting (right panel) AMPT model for Pb+Pb collisions at $\sqrt{s_{NN}} = 2.76$ TeV and impact parameter $b = 8$ fm. It is seen that the B_2 for ^{2}H-like nuclei as well as the B_3 for both ^{3}H-like and $^3_\Lambda$H-like nuclei increase with increasing transverse momentum in both the default and string melting AMPT model, similar to that extracted from the experimental data from the ALICE Collaboration [1,2] shown by open squares for B_2 and open circles for B_3. Their values at low p_T are a few times 10^{-3} GeV$^2/c^3$ for B_2 and about 10^{-6} GeV$^4/c^6$ for B_3 with that for ^{3}H-like nuclei slightly larger than that for $^3_\Lambda$H-like nuclei. Compared to the experimentally extracted values from the ALICE Collaboration, the default AMPT gives a B_2 that is about a factor of two larger and a B_3 that is about a factor of two smaller. For the string melting AMPT model, the obtained B_2 is about a factor of two larger at lower momentum and almost an order of magnitude larger at higher momentum than the empirical value, although it gives a B_3 that agrees with the empirical one.

V. SUMMARY

We have studied in the present paper the production of light normal and hypernuclei and their antinuclei in heavy-ion collisions at the LHC by using the coalescence model. With the phase-space distributions of protons, neutrons, and Λs as well as their antiparticles at freeze-out taken from the AMPT model, and taking the Wigner functions of these nuclei to be of Gaussian form with their width parameters fitted to their known charge radii, we have calculated the transverse momentum spectra and elliptic flows of ^{2}H-like nuclei that include ^{2}H and $^2\bar{\text{H}}$, of ^{3}H-like nuclei that include ^{3}H, ^{3}He, $^3\bar{\text{H}}$, and $^3\overline{\text{He}}$, and of $^3_\Lambda$H-like nuclei that include $^3_\Lambda$H, $^3_\Lambda$He, $^3_\Lambda n$, $^3_{\bar{\Lambda}}\bar{\text{H}}$, $^3_{\bar{\Lambda}}\overline{\text{He}}$, and $^3_{\bar{\Lambda}}\bar{n}$.

For the transverse momentum spectra, we have found that the default version of the AMPT model gives a better description of the experimental data from the ALICE Collaboration for proton and deuteron than the string melting version of

the AMPT model, and this has been attributed to the baryon problem in the current string melting version of the AMPT code. From the total yield of these nuclei, we have verified the experimental observation that the yield of light nuclei is reduced by about two orders of magnitude with the addition of a nucleon or Λ to a nucleus.

For the elliptic flows of these nuclei, they are found to show a mass ordering behavior with the heavy nuclei having a smaller elliptic flow, like that in the hydrodynamical description of heavy-ion collisions. This behavior is seen in both the default and the string melting AMPT model. We have further found that the elliptic flows of light nuclei display an approximate constituent number scaling in that their elliptic flows at transverse momentum p_T per constituent are the same as a function of p_T divided by the number of constituents, particularly in the case of the default AMPT model.

We have further studied the coalescence parameter B_A for light nuclei, which is defined by the ratio of the invariant transverse momentum spectrum of a nucleus to that of its constituents raised to the power corresponding to the number of constituents in the nucleus. Our results based on both the default and string melting AMPT models indicate that the coalescence parameter increases with increasing transverse momentum of a nucleus, similar to that extracted from the experimental data. Their values are, however, a factor of two larger for B_2 and a factor of two smaller for B_3 in the case of the default AMPT model. In the string melting version of the AMPT model, the value of B_2 is almost an order of magnitude larger than data at high momentum but that of B_3 agrees with the data.

Although our results are qualitatively comparable to the experimental data from the LHC, they do not give a quantitative description, particularly in the case of the string melting version of the AMPT model due to its problem in treating baryon production during hadronization. Since it is known that a strongly interacting partonic stage exists in relativistic heavy-ion collisions, an improved description of baryon production in the AMPT model is urgently needed in order to study quantitatively light nuclei production in relativistic heavy-ion collisions.

Also, the elliptic flows of light nuclei that are produced via the coalescence model are always positive, even though they do show a mass ordering as in the hydrodynamic approach. Since masses of these light nuclei are comparable to that of a charmonium, which has been shown to have a negative elliptic flow in the hydrodynamic description of relativistic heavy-ion collisions [41], we expect that the light nuclei studied here would have negative elliptic flows as well if they are produced statistically in the hydrodynamic model. Therefore, it is of great interest to measure experimentally the elliptic flows of light nuclei to see if they are positive like in the coalescence model or negative as in the hydrodynamic model.

ACKNOWLEDGMENTS

We thank Lie-Wen Chen, Su Houng Lee, Zie-Wei Lin, Yongseok Oh, and Jun Xu for helpful communications and/or discussions. We are further indebted to Yu-Gang Ma for his critical comments and suggestions. One of the authors (C.M.K.) is grateful to the Physics Department at Sichuan University for the warm hospitality during his visit when this work was carried out. This work was supported in part by the NSFC of China under Grant No. 11205106 and the Welch Foundation under Grant No. A-1358.

[1] J. Adam *et al.* (ALICE Collaboration), arXiv:1506.08951 [nucl-ex].
[2] J. Adam *et al.* (ALICE Collaboration), arXiv:1506.08453 [nucl-ex].
[3] C. Adler *et al.* (STAR Collaboration), Phys. Rev. Lett. **87**, 262301 (2001).
[4] B. I. Abelev *et al.* (STAR Collaboration), arXiv:0909.0566 [nucl-ex].
[5] B. I. Abelev (STAR Collaboration), Science **328**, 58 (2010).
[6] H. Agakishiev *et al.* (STAR Collaboration), Nature (London) **473**, 353 (2011).
[7] G. Bertsch, M. Gong, and M. Tohyama, Phys. Rev. C **37**, 1896 (1988).
[8] S. Pratt, T. Csorgo, and J. Zimanyi, Phys. Rev. C **42**, 2646 (1990).
[9] M. Gyulassy, K. Frankel, and E. A. Remler, Nucl. Phys. A **402**, 596 (1983).
[10] J. Aichelin, A. Rosenhauer, G. Peilert, H. Stoecker, and W. Greiner, Phys. Rev. Lett. **58**, 1926 (1987).
[11] V. Koch, B. Blättle, W. Cassing, U. Mosel, and K. Weber, Phys. Lett. B **241**, 174 (1990).
[12] P. Pawlowski *et al.*, Eur. Phys. J. A **9**, 371 (2000).
[13] R. Mattiello, H. Sorge, H. Stöcker, and W. Greiner, Phys. Rev. C **55**, 1443 (1997).
[14] J. L. Nagle, B. S. Kumar, D. Kusnezov, H. Sorge, and R. Mattiello, Phys. Rev. C **53**, 367 (1996).
[15] G. Chen, Y. L. Yan, D. S. Li, D. M. Zhou, M. J. Wang, B. G. Dong, and B. H. Sa, Phys. Rev. C **86**, 054910 (2012).
[16] G. Chen, H. Chen, J. Wu, D. S. Li, and M. J. Wang, Phys. Rev. C **88**, 034908 (2013).
[17] S. Zhang, J. H. Chen, H. Crawford, D. Keane, Y. G. Ma, and Z. B. Xu, Phys. Lett. B **684**, 224 (2010).
[18] K. J. Sun and L. W. Chen, Phys. Lett. B **751**, 272, 2015.
[19] Z. L. She, G. Chen, H. G. Xu, and T. T. Zeng, arXiv:1509.06493 [nucl-th].
[20] L. W. Chen, C. M. Ko, and B. A. Li, Phys. Rev. C **68**, 017601 (2003).
[21] L. W. Chen, C. M. Ko, and B. A. Li, Nucl. Phys. A **729**, 809 (2003).
[22] Y. Oh, Z. W. Lin, and C. M. Ko, Phys. Rev. C **80**, 064902 (2009).
[23] Z. W. Lin, C. M. Ko, B. A. Li, B. Zhang, and S. Pal, Phys. Rev. C **72**, 064901 (2005).
[24] X. N. Wang and M. Gyulassy, Phys. Rev. D **44**, 3501 (1991).
[25] B. Zhang, Comput. Phys. Commun. **109**, 193 (1998).
[26] B. A. Li and C. M. Ko, Phys. Rev. C **52**, 2037 (1995).
[27] J. Xu and C. M. Ko, Phys. Rev. C **83**, 034904 (2011).

[28] A. Andronic, P. Braun-Munzinger, J. Stachel, and H. Stocker, Phys. Lett. B **697**, 203 (2011).
[29] J. Cleymans, S. Kabana, I. Kraus, H. Oeschler, K. Redlich, and N. Sharma, Phys. Rev. C **84**, 054916 (2011).
[30] C. M. Ko, T. Song, F. Li, V. Greco, and S. Plumari, Nucl. Phys. A **928**, 234 (2014).
[31] I. Angeli and K. P. Marinova, At. Data Nucl. Data Tables **99**, 69 (2013).
[32] C. Rappold, E. Kim, T. R. Saito, O. Bertini, S. Bianchin, V. Bozkurt, M. Kavatsyuk, Y. Ma, F. Maas, S. Minami, D. Nakajima, B. Ozel-Tashenov, K. Yoshida, P. Achenbach, S. Ajimura, T. Aumann, C. AyerbeGayoso, H. C. Bhang, C. Caesar, S. Erturk, T. Fukuda, B. Gokuzum, E. Guliev, J. Hoffmann, G. Ickert, Z. S. Ketenci, D. Khaneft, M. Kim, S. Kim, K. Koch, N. Kurz, A. LeFevre, Y. Mizoi, L. Nungesser, W. Ott, J. Pochodzalla, A. Sakaguchi, C. J. Schmidt, M. Sekimoto, H. Simon, T. Takahashi, G. J. Tambave, H. Tamura, W. Trautmann, S. Voltz, and C. J. Yoon (HypHI Collaboration), Phys. Rev. C **88**, 041001 (2013).
[33] S. Cho, T. Furumoto, T. Hyodo, D. Jido, C. M. Ko, S. H. Lee, M. Nielsen, A. Ohnishi, T. Sekihara, S. Yasui, and K. Yazaki (ExHIC Collaboration), Phys. Rev. C **84**, 064910 (2011).
[34] G. Bertsch, M. Gong, L. D. McLerran, P. V. Ruuskanen, and E. Sarkkinen, Phys. Rev. D **37**, 1202 (1988).
[35] S. I. Gogolev *et al.*, Phys. Lett. B **300**, 24 (1993).
[36] E. A. Pasyuk, V. Y. Alexakhin, S. I. Gogolev, K. O. Oganesyan, C. L. Morris, J. M. O'Donnell, M. W. Rawool-Sullivan, M. K. Jones, F. F. Guber, A. I. Reshetin, and I. I. Strakovsky, Phys. Rev. C **55**, 1026 (1997).
[37] D. Molnar and S. A. Voloshin, Phys. Rev. Lett. **91**, 092301 (2003).
[38] P. F. Kolb, L. W. Chen, V. Greco, and C. M. Ko, Phys. Rev. C **69**, 051901 (2004).
[39] L. W. Chen and C. M. Ko, Phys. Rev. C **73**, 044903 (2006).
[40] T. Z. Yan *et al.*, Phys. Lett. B **638**, 50 (2006).
[41] T. Song, C. M. Ko, S. H. Lee, and J. Xu, Phys. Rev. C **83**, 014914 (2011).